Aging model for Meteosat First Generation VIS Band

Ilse Decoster, N. Clerbaux, E. Baudrez, S. Dewitte, A. Ipe, S. Nevens, A. Velazquez Blazquez, J. Cornelis

Royal Meteorological Institute of Belgium (RMIB)
Satellite Application Facility on Climate Monitoring (CM SAF)
Vrije Universiteit Brussel (VUB)

Earth Radiation Budget Workshop
22 - 25 October 2012, GFDL, Princeton, NJ (USA)

Outline

Timeline Meteosat Satellites: 1977 - 2011

- MFG carrying narrow band imager MVIRI
- MSG carrying narrow band imager SEVIRI + broad band imager GERB

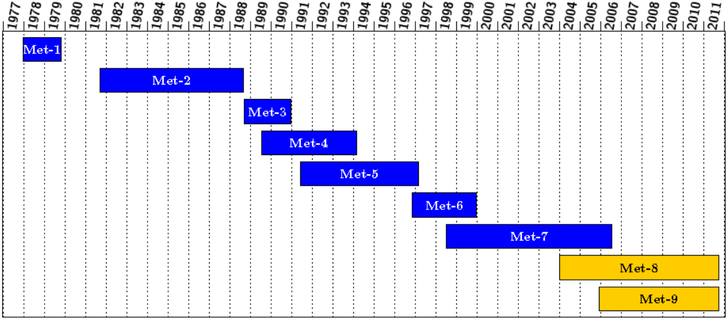

Figure : *Operational time around 0° for Meteosat satellites*

$\Rightarrow$ 25 years of MVIRI data at 0° longitude

Meteosat VIS and IR Imager (MVIRI)

MVIRI : **M**eteosat **V**isible and **I**nfra **R**ed **I**mager

- 1 image every 30 minutes
- 3 spectral channels:
  visible (VIS), water vapour (WV), infra red (IR)

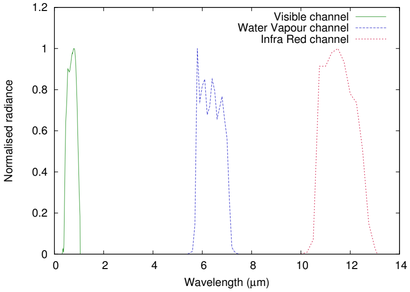

Figure : *Normalized spectral response curves for MVIRI channels (given here are the curves for Meteosat-7)*

Meteosat First Generation (MFG)

Long data records: **climatology**

⇒ EUMETSAT created Climate Monitoring Satellite Application Facility (CM SAF) in 1999

Usefulness of

- Fundamental Climate Data Records (FCDRs)
- Thematic Climate Data Records (TCDRs)
  aerosol, precipitation, albedo, cloud properties, etc.

Global Climate Observing System (GCOS) setting limits on e.g. stability of DRs

⇒ Calibration: good and consistent over entire record!

Calibration of VIS channel

Current EUMETSAT calibration method for VIS band: constantly increasing calibration coefficient in time

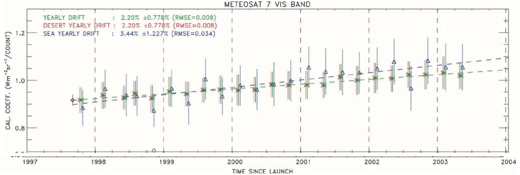

Figure : *Calibration coefficient Meteosat-7 (Govaerts et al. 2004).*

Validation of this method: in-flight change of the spectral response with stronger degradation effect for shorter wavelengths: **spectral darkening**

Spectral darkening

Probable reason of degradation process of the visible channel:

- Instruments in space: **outgassing** of lightweight molecules (moisture, lubricants, adhesives, etc.)
- Outgassed material **condenses** onto surface of the mirrors of the instruments
- When material is exposed to UV-radiation from Sun: **photodeposition** on the mirrors
- On top, energy from Sun changes optical properties of deposited material

Result: stronger absorption in shorter VIS wavelengths than in longer:

spectral darkening

Outline

Spectral response function

In this work the calibration coefficient was kept constant at the value at launch (unlike the EUMETSAT method) and the **temporal variation of the spectral response** was modeled:

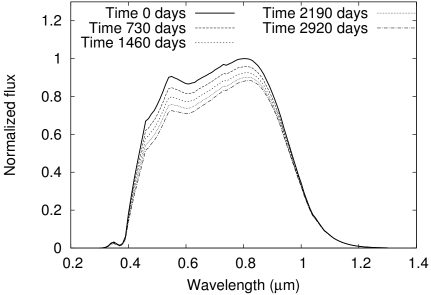

Figure : *Spectral response curve of Meteosat-7 with aging correction after several time steps.*

Modeled spectral response function

$$\phi(\lambda, t) = \phi(\lambda, 0)\,(e^{-\alpha\, t} + \beta\,(1 - e^{-\alpha\, t}))\,(1 + \gamma\, t\,(\lambda - \lambda_0))$$

- Gray degradation: $e^{-\alpha\, t} + \beta\,(1 - e^{-\alpha\, t})$
  - α: decay rate of gray degradation
  - β: asymptotic sensitivity when t $\rightarrow \infty$
- Spectral degradation: $1 + \gamma\, t\,(\lambda - \lambda_0)$
  - γ: decay rate of spectral degradation

Outline

Meteosat-7 data used

- Model has been tested using only Meteosat-7 data
- One image a day is used at noon (12:00 UTC if available, else the one at 11:00 UTC or 13:00 UTC)
- Data period used is from June 3, 1998 until June 11, 2006

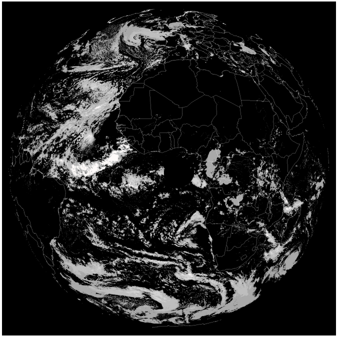

From digital count to reflectance ratio

Images are converted into reflectance ratio:

- **Value** v of original images in digital counts $[DC]$
- **Radiance** $L = C_f \, . \, (v - O)$ $[W/(m^2 \, sr)]$
  with C_f and O the fixed calibration coefficient and offset (EUMETSAT calibration)

  = **Narrowband Radiance:** $L = \int_{\text{VIS}} L(\lambda)\phi(\lambda)d\lambda$
  with $L(\lambda)$ the spectral radiance at wavelength λ and $\phi(\lambda)$ the spectral response of the instrument
- **Narrowband Reflectance** $\rho = L \, / \left(\frac{FSI \, . \, cos(\theta_0)}{\pi \, . \, d^2} \right)$
  with θ_0 the solar zenith angle, d the Sun - Earth distance in AU, and FSI the Filtered Solar Irradiance

From digital count to reflectance ratio

Images are converted into reflectance ratio:

- **Value** v of original images in digital counts $[DC]$
- **Radiance** $L = C_f \, . \, (\, v - O)$ $[W/(m^2 \, sr)]$
  with C_f and O the fixed calibration coefficient and offset (EUMETSAT calibration)

  $=$ **Narrowband Radiance:** $L = \int_{\text{VIS}} L(\lambda)\phi(\lambda)d\lambda$
  with $L(\lambda)$ the spectral radiance at wavelength λ and $\phi(\lambda)$ the spectral response of the instrument
- **Narrowband Reflectance** $\rho = L \, / \left(\frac{FSI \, . \, cos(\theta_0)}{\pi \, . \, d^2} \right)$
  with θ_0 the solar zenith angle, d the Sun - Earth distance in AU, and FSI the Filtered Solar Irradiance

From digital count to reflectance ratio

Images are converted into reflectance ratio:

- **Value** v of original images in digital counts $[DC]$
- **Radiance** $L = C_f \,.\, (\, v - O)$ $[W/(m^2\, sr)]$
  with C_f and O the fixed calibration coefficient and offset (EUMETSAT calibration)

  $=$ **Narrowband Radiance:** $L = \int_{\text{VIS}} L(\lambda)\phi(\lambda)d\lambda$
  with $L(\lambda)$ the spectral radiance at wavelength λ and $\phi(\lambda)$ the spectral response of the instrument
- **Narrowband Reflectance** $\rho = L \,/\, \left(\frac{FSI \,.\, \cos(\theta_0)}{\pi \,.\, d^2} \right)$
  with θ_0 the solar zenith angle, d the Sun - Earth distance in AU, and FSI the Filtered Solar Irradiance

From digital count to reflectance ratio

Images are converted into reflectance ratio:

- **Value** v of original images in digital counts $[DC]$
- **Radiance** $L = C_f \,.\, (\, v - O)$ $[W/(m^2\, sr)]$
  with C_f and O the fixed calibration coefficient and offset (EUMETSAT calibration)

  $=$ **Narrowband Radiance:** $L = \int_{\mathrm{VIS}} L(\lambda)\phi(\lambda)d\lambda$
  with $L(\lambda)$ the spectral radiance at wavelength λ and $\phi(\lambda)$ the spectral response of the instrument
- **Narrowband Reflectance** $\rho = L \,/\, \left(\frac{FSI \,.\, \cos(\theta_0)}{\pi \,.\, d^2}\right)$
  with θ_0 the solar zenith angle, d the Sun - Earth distance in AU, and FSI the Filtered Solar Irradiance

From digital count to reflectance ratio (2)

- **Broadband reflectance** $\rho_{BB} = a + b\,\rho$
  → simulate spectral radiances $L(\lambda)$ leading to simulated narrowband and broadband radiances:

$$L = \int_{VIS} L(\lambda)\phi(\lambda,0)\,(e^{-\alpha t} + \beta\,(1 - e^{-\alpha t}))\,(1 + \gamma\,t\,(\lambda - \lambda_0))d\lambda$$

$$L_{BB} = \int_{0-2\mu m} L(\lambda)d\lambda$$

  → convert to reflectance and compute a and b coefficients for different surface types and cloudiness

  → convert observed reflectance to broad band reflectance using these values

- **Reflectance ratio** $r = \frac{\rho_{BB}}{R(\theta_0,\theta,\psi)\,.\,Alb(\theta_0)}$
  with R the modeled anisotropy factor, θ_0 the solar zenith angle, θ the viewing zenith angle, ψ the relative azimuth angle and Alb the albedo

From digital count to reflectance ratio (2)

- **Broadband reflectance** $\rho_{BB} = a + b\,\rho$

  $\rightarrow$ simulate spectral radiances $L(\lambda)$ leading to simulated narrowband and broadband radiances:

$$L = \int_{\mathrm{VIS}} L(\lambda)\phi(\lambda,0)\,(e^{-\alpha\,t} + \beta\,(1 - e^{-\alpha\,t}))\,(1 + \gamma\,t\,(\lambda - \lambda_0))d\lambda$$

$$L_{BB} = \int_{0\text{–}2\mu\mathrm{m}} L(\lambda)d\lambda$$

  $\rightarrow$ convert to reflectance and compute a and b coefficients for different surface types and cloudiness

  $\rightarrow$ convert observed reflectance to broad band reflectance using these values

- **Reflectance ratio** $r = \frac{\rho_{BB}}{R(\theta_0,\theta,\psi)\,.\,Alb(\theta_0)}$

  with R the modeled anisotropy factor, θ_0 the solar zenith angle, θ the viewing zenith angle, ψ the relative azimuth angle and Alb the albedo

From digital count to reflectance ratio (2)

- **Broadband reflectance** $\rho_{BB} = a + b\,\rho$
  $\rightarrow$ simulate spectral radiances $L(\lambda)$ leading to simulated narrowband and broadband radiances:

$$L = \int_{\mathrm{VIS}} L(\lambda)\phi(\lambda, 0)\,(e^{-\alpha\,t} + \beta\,(1 - e^{-\alpha\,t}))\,(1 + \gamma\,t\,(\lambda - \lambda_0))d\lambda$$

$$L_{BB} = \int_{0\text{–}2\mu\mathrm{m}} L(\lambda)d\lambda$$

  $\rightarrow$ convert to reflectance and compute a and b coefficients for different surface types and cloudiness

  $\rightarrow$ convert observed reflectance to broad band reflectance using these values

- **Reflectance ratio** $r = \frac{\rho_{BB}}{R(\theta_0,\theta,\psi)\,.\,Alb(\theta_0)}$
  with R the modeled anisotropy factor, θ_0 the solar zenith angle, θ the viewing zenith angle, ψ the relative azimuth angle and Alb the albedo

From digital count to reflectance ratio (2)

- **Broadband reflectance** $\rho_{BB} = a + b\,\rho$
  $\rightarrow$ simulate spectral radiances $L(\lambda)$ leading to simulated narrowband and broadband radiances:

$$\begin{aligned} L &= \int_{\text{VIS}} L(\lambda)\phi(\lambda,0)\,(e^{-\alpha\,t} + \beta\,(1-e^{-\alpha\,t})) \\ &\qquad (1+\gamma\,t\,(\lambda-\lambda_0))d\lambda \\ L_{BB} &= \int_{0\text{–}2\mu\text{m}} L(\lambda)d\lambda \end{aligned}$$

  $\rightarrow$ convert to reflectance and compute a and b coefficients for different surface types and cloudiness

  $\rightarrow$ convert observed reflectance to broad band reflectance using these values

- **Reflectance ratio** $r = \frac{\rho_{BB}}{R(\theta_0,\theta,\psi)\,.\,Alb(\theta_0)}$
  with R the modeled anisotropy factor, θ_0 the solar zenith angle, θ the viewing zenith angle, ψ the relative azimuth angle and Alb the albedo

From digital count to reflectance ratio (2)

- **Broadband reflectance** $\rho_{BB} = a + b\,\rho$

  $\rightarrow$ simulate spectral radiances $L(\lambda)$ leading to simulated narrowband and broadband radiances:

  $$L = \int_{VIS} L(\lambda)\phi(\lambda,0)\,(e^{-\alpha\,t} + \beta\,(1 - e^{-\alpha\,t}))\,(1 + \gamma\,t\,(\lambda - \lambda_0))d\lambda$$

  $$L_{BB} = \int_{0-2\mu m} L(\lambda)d\lambda$$

  $\rightarrow$ convert to reflectance and compute a and b coefficients for different surface types and cloudiness

  $\rightarrow$ convert observed reflectance to broad band reflectance using these values

- **Reflectance ratio** $r = \frac{\rho_{BB}}{R(\theta_0,\theta,\psi)\,.\,Alb(\theta_0)}$

  with R the modeled anisotropy factor, θ_0 the solar zenith angle, θ the viewing zenith angle, ψ the relative azimuth angle and Alb the albedo

Selecting stable targets

To model the parameters, different targets in the Meteosat FOV are needed

- Both cloudy and clear-sky targets
- Clear-sky targets:
  - Need clear-sky images: every 10 days pixel to pixel analysis of series of 30 images before and 30 images leads to clear-sky image (Ipe et al. (2003))
  - Different scene types used: bright vegetation, dark vegetation, bright desert, dark desert and ocean
- Look for **stable sites**:
  - stable clear-sky sites have lowest standard deviation in the total series of images
  - stable cloudy sites are chosen amongst the highly convective clouds, so the highest reflectance values

Selecting stable targets

To model the parameters, different targets in the Meteosat FOV are needed

- Both cloudy and clear-sky targets
- Clear-sky targets:
  - Need clear-sky images: every 10 days pixel to pixel analysis of series of 30 images before and 30 images leads to clear-sky image (Ipe et al. (2003))
  - Different scene types used: bright vegetation, dark vegetation, bright desert, dark desert and ocean
- Look for **stable sites**:
  - stable clear-sky sites have lowest standard deviation in the total series of images
  - stable cloudy sites are chosen amongst the highly convective clouds, so the highest reflectance values

Selecting stable targets

To model the parameters, different targets in the Meteosat FOV are needed

- Both cloudy and clear-sky targets
- Clear-sky targets:
  - Need clear-sky images: every 10 days pixel to pixel analysis of series of 30 images before and 30 images leads to clear-sky image (Ipe et al. (2003))
  - Different scene types used: bright vegetation, dark vegetation, bright desert, dark desert and ocean
- Look for **stable sites**:
  - stable clear-sky sites have lowest standard deviation in the total series of images
  - stable cloudy sites are chosen amongst the highly convective clouds, so the highest reflectance values

Selecting stable targets

To model the parameters, different targets in the Meteosat FOV are needed

- Both cloudy and clear-sky targets
- Clear-sky targets:
  - Need clear-sky images: every 10 days pixel to pixel analysis of series of 30 images before and 30 images leads to clear-sky image (Ipe et al. (2003))
  - Different scene types used: bright vegetation, dark vegetation, bright desert, dark desert and ocean
- Look for **stable sites**:
  - stable clear-sky sites have lowest standard deviation in the total series of images
  - stable cloudy sites are chosen amongst the highly convective clouds, so the highest reflectance values

Creating time series

- Residual seasonal correction
- Averaging of targets according to scene type

$\Rightarrow$ 6 time series:

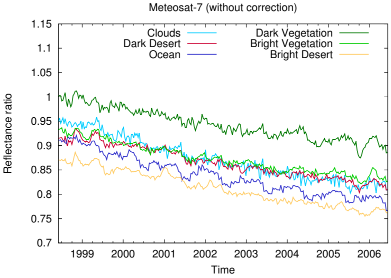

surface type	broadband slope (% yr^{-1})
convective clouds	-1.9090 ± 0.0230
ocean	-1.7900 ± 0.0222
dark vegetation	-1.2542 ± 0.0204
bright vegetation	-1.3895 ± 0.0167
dark desert	-1.5328 ± 0.0156
bright desert	-1.6847 ± 0.0149
weighted average	-1.8176

Minimization technique

Find parameters (α, β, γ) that minimize variance of time series:

1. Simulate the spectral radiance $L(\lambda)$ for different surface types and cloudiness
2. Set the model parameters (α, β, γ) to an initial value
3. Calculate L and L_{BB} with the given parameter values
4. Convert the simulated radiances into reflectances
5. Do the NB to BB conversion, fitting the a and b values for these simulated reflectance values
6. Use the values for a and b from this conversion to convert the observed reflectance ρ to broadband reflectance ρ_{BB}
7. Transform ρ_{BB} to reflectance ratio r

Minimization technique (2)

8. Minimize the variance

$$\sum_{i=1}^{6} w_i \left(\frac{1}{N} \left(\sum_{j=1}^{N} r_{ij}^2 - \frac{\left(\sum_{j=1}^{N} r_{ij} \right)^2}{N} \right) \right)$$

using the method of Powell et al. (1964) and using these r values.

9. If the cost function does not lead to the optimal solution, the Powell method returns a new set of (α, β, γ) parameters and the routine goes back to step 3.

Corrected time series Meteosat-7

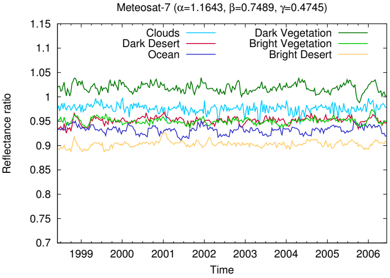

surface type	broadband slope (% yr^{-1})
convective clouds	-0.0463 ± 0.0181
ocean	-0.0105 ± 0.0166
dark vegetation	-0.0605 ± 0.0190
bright vegetation	0.0030 ± 0.0129
dark desert	0.0758 ± 0.0147
bright desert	0.0623 ± 0.0132
weighted average	-0.0267

parameter	optimal solution	standard deviation
gray decay rate α	1.1643 / decade	0.1606 / decade
asymptotic sensitivity β	0.7489	0.0161
spectral decay rate γ	0.4745 μm^{-1} / decade	0.0329 μm^{-1} / decade

Outline

Regional validation

Narrowband to broadband conversion before was done using clear-sky simulations for clear-sky targets and convective cloud simulations for the cloudy targets

For validation:

- **allsky** simulated spectral radiances $L(\lambda)$ are used to compute a and b values
- no allsky R and Alb values, so **no conversion to reflectance ratio**

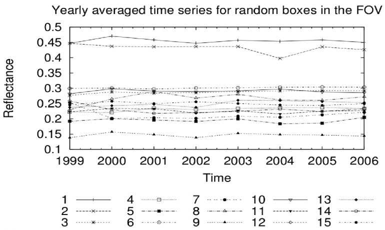

(a)

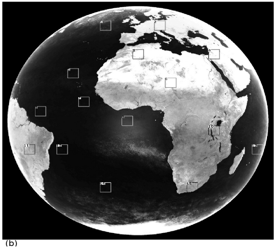

(b)

Regional Validation (2)

Validation done on both original and clear-sky images:

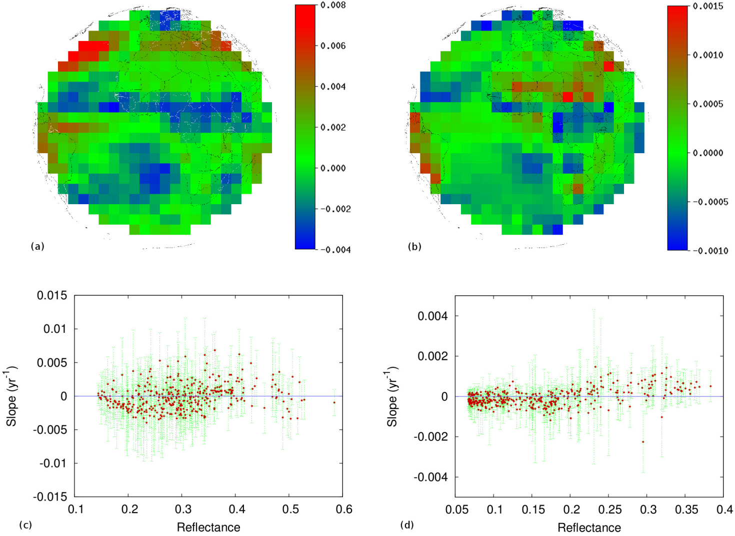

IGBP surface type selection

Instead of grouping targets in 6 groups, the 17 class land cover dataset of IGBP is used

number	name	% of sites in FOV	slope (yr^{-1})	χ_{red}
1	Evrgr. Needleleaf For.	0.505	$2.5 \,.\, 10^{-4}$	$9.35 \,.\, 10^{-3}$
2	Evrgr. Broadleaf For.	0.440	$4.0 \,.\, 10^{-6}$	$1.40 \,.\, 10^{-3}$
3	Decid. Needleleaf For.	0.003	$1.3 \,.\, 10^{-4}$	$2.37 \,.\, 10^{-2}$
4	Decid. Broadleaf For.	0.250	$1.3 \,.\, 10^{-5}$	$1.41 \,.\, 10^{-3}$
5	Mixed Forest	0.146	$1.2 \,.\, 10^{-4}$	$2.94 \,.\, 10^{-3}$
6	Closed Shrublands	0.763	$-3.0 \,.\, 10^{-6}$	$1.04 \,.\, 10^{-3}$
7	Open Shrublands	2.874	$3.9 \,.\, 10^{-5}$	$9.23 \,.\, 10^{-4}$
8	Woody Savannas	4.162	$-1.3 \,.\, 10^{-5}$	$1.49 \,.\, 10^{-3}$
9	Savannas	5.698	$1.6 \,.\, 10^{-5}$	$1.07 \,.\, 10^{-3}$
10	Grassland	2.262	$5.4 \,.\, 10^{-5}$	$1.42 \,.\, 10^{-3}$
11	Permanent Wetlands	0.070	$1.9 \,.\, 10^{-4}$	$3.51 \,.\, 10^{-3}$
12	Croplands	2.273	$1.2 \,.\, 10^{-5}$	$1.77 \,.\, 10^{-3}$
13	Urban and Built-up	0.021	$1.4 \,.\, 10^{-5}$	$1.64 \,.\, 10^{-3}$
14	Cropland Mosaics	4.415	$3.3 \,.\, 10^{-5}$	$1.01 \,.\, 10^{-3}$
16	Bare Soil and Rocks	9.601	$3.0 \,.\, 10^{-5}$	$1.14 \,.\, 10^{-3}$
17	Water Bodies	62.26	$-3.0 \,.\, 10^{-6}$	$8.57 \,.\, 10^{-4}$

Comparison EUMETSAT model

To compare results, the same 6 time series are corrected using the method of Y. Govaerts

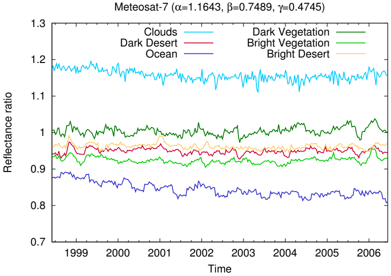

surface type	EUMETSAT slope (% yr^{-1})
convective clouds	-0.2689 ± 0.0263
ocean	-0.7562 ± 0.0238
dark vegetation	0.1219 ± 0.0234
bright vegetation	-0.0139 ± 0.0183
dark desert	-0.0320 ± 0.0165
bright desert	-0.1011 ± 0.0154
weighted average	-0.3044

Outline

Paper has been accepted for publication in JAOT (AMS)

A spectral aging model for the Meteosat-7 visible band

I. DECOSTER *

Royal Meteorological Institute of Belgium, Brussels, Belgium

Vrije Universiteit Brussel, Brussels, Belgium

N. CLERBAUX, E. BAUDREZ , S. DEWITTE, A. IPE, S. NEVENS AND A. VELAZQUEZ BLAZQUEZ

Royal Meteorological Institute of Belgium, Brussels, Belgium

J. CORNELIS

Vrije Universiteit Brussel, Brussels, Belgium

ABSTRACT

Since more than 30 years, the Meteosat satellites are in a geostationary orbit around the Earth. Due to the high temporal frequency of the data and the long time period, this database is an excellent candidate for Fundamental Climate Data Records (FCDRs). One of the prerequisites to create FCDRs is an accurate and stable calibration over the full data period. Due to the presence of contamination on the instrument in space, a degradation of the visible band of the instruments has been observed. Previous work on the Meteosat First Generation satellites, together with results from other spaceborne instruments, lead to the idea that there is a spectral component to this degradation. This paper describes the model that is created to correct the Meteosat-7 VIS channel for these spectral aging effects. The model assumes an exponential temporal decay for the gray part of the degradation and a linear temporal decay for the wavelength-dependent part. The effect of these two parts of the model is tuned according to three parameters. 253 clearsky stable Earth targets with different surface types are used together with deep convective cloud measurements to fit these parameters. The validation of the model leads to an overall stability of the Meteosat-7 reflected solar radiation data record of about 0.66 $\mathrm{W\,m^{-2}}$ / decade.

Next steps ...

- The model is being applied to rest of MFG, but countering lots of difficulties (volcanic erruptions in data, time series too short to get parameters or do deseasonalization, etc.)
- Getting more data from EUMETSAT, use the ADC, XADC, IODC to extend databases
- Check applications of new model for GERB-like data, aerosols, surface albedo, etc.
- Full MFG database will be reprocessed by 2015, using this model to correct for degradation of the VIS channel